How to Predict the Sound Spectrum of a Helmholtz Resonator under Grazing Turbulent Flow

Lewin Stein[1], Jörn Sesterhenn[1]

[1] *Institut für Strömungsmechanik und Technische Akustik, 10623 Berlin, Deutschland, Email: lewin.stein@tu-berlin.de*

Introduction

Perforated linings backed by arrays of Helmholtz resonators are well-established as silencers of tonal noise in turbulent flow. Areas of application are intake and exhaust ducts of combustion engines or jet engines. Due to a complex turbulence-acoustic interaction, the layout of such linings depends on expansive experimental test series. So far there is a lack of easy applicably but realistic sound absorption models. If the streamwise extension of the opening is smaller than the boundary layer thickness the turbulence-acoustic interaction is minimized. Thus up to now, most sound prediction models are restricted to an acoustical description only. In the present case, the opening is larger than the boundary layer thickness. This implies the development of an unstable shear layer at the opening, which can be exploited as additional silencing mechanism, as shown in this work.

Typically, Liners operate at subsonic and low-frequency conditions near the Helmholtz base frequency far below the cutoff frequency of higher cavity modes. We exploit the confined range of operation to set up a model for a single Helmholtz resonator under grazing turbulent flow. The model will be contrasted with a Direct Numerical Simulation (DNS) and with an experiment. Based on the model predictions are made: Without flow, the resistance is always positive. With flow the Helmholtz resonator can act both as a silencer or as an amplifier: At low frequency, the shear layer absorbs acoustic energy; on the contrary at higher frequencies tones occur.

Studied Case

The elementary element of a Liner studied here consists of a turbulent flat plate flow on top and a rectangular cavity below. The cavity is joined via a rectangular opening/neck with the flat plate. Since the neck volume is much smaller than the volume of the cavity the classical idealization of a Helmholtz Resonator is effectual. A sketch of the geometry is provided in figure 1.

To gain information about all flow variables at all times in a fully controlled manner, without any experimental restriction and without any simplification of the nonlinear turbulence-acoustic interaction we conducted first a DNS. The dataset of this DNS allows to identify major and minor mechanisms and such legitimates the later model assumptions.

The characteristic parameters of our reference DNS are a Reynolds number of $Re_{\delta_{99,neck}} \sim 4200$ at the upstream edge of the neck; and a low Mach number of $M \sim 0.1$ which corresponds to a free stream velocity

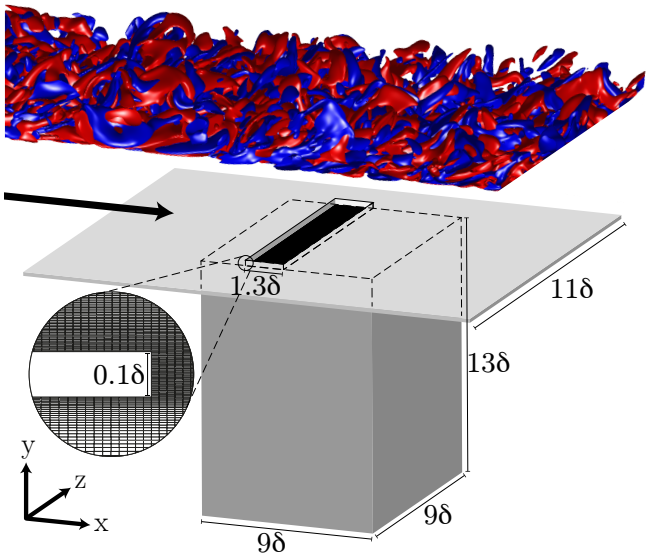

Figure 1: Setup of the studied Helmholtz resonator under grazing turbulent flow. All units are given in terms of the boundary layer thickness δ_{99}, defined at the upstream opening edge $\delta_{99,neck} \cong 1$cm.

of $u_0 \sim 40$m/s. In order to simulate ~ 30ms of physical time $\sim 3.6 \times 10^6$ CPU-hours were used with a structured grid composed of 1.2×10^9 grid points. Near the opening, the grid was further refined as indicated in figure 1. A fully conservative, acoustically optimized formulation of the compressible Navier-Stokes equation was computed with our well established in-house finite-difference solver [8, 7, 9]. In space and time, fourth order schemes are applied.

Results

Derivation of the Sound Prediction Model

The sound prediction model assumes separable acoustical and fluid dynamical phenomena. The acoustical part is based on linear, **lumped, acoustic elements** [6]. The fluid dynamical part is based on a pressure source term and the **Howe model**. The model itself is a transfer function which relates the pressure spectrum of the driving turbulent boundary layer (denoted by the red dot of figure 2) with the pressure spectrum at the bottom of the cavity (green dot of figure 2) Details of the sound prediction model derivation are given in [2].

In here we focus on the Howe model only. The Howe model is the most crucial part of the final sound prediction model, since here the energy interchange between the turbulent flow and the acoustics takes place.

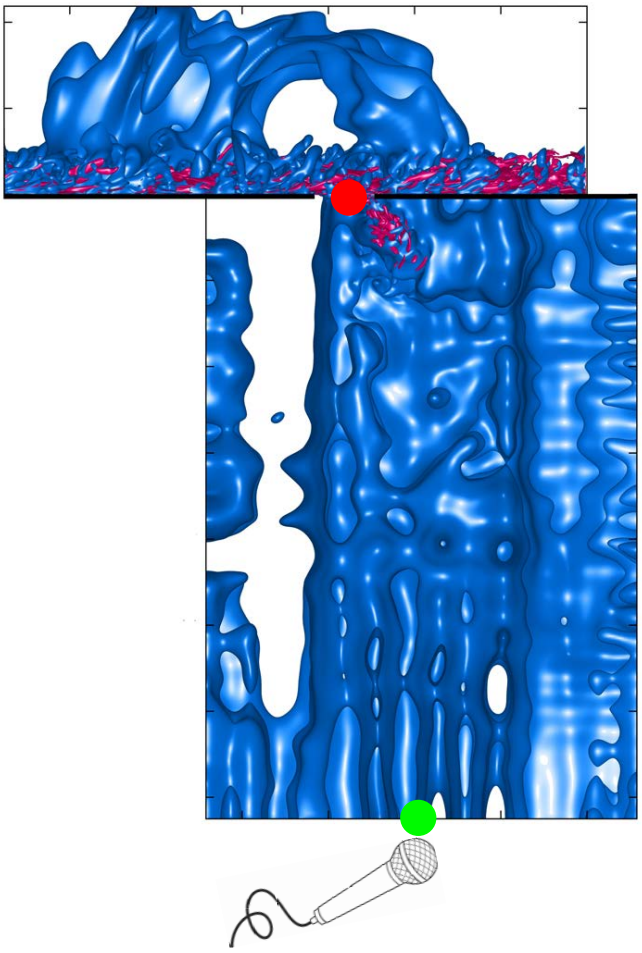

Figure 2: Snapshot of isosurfaces of pressure (blue) and vorticity (pink). At the top the turbulent boundary layer is visible. Below the rectangular cavity of the Helmholtz resonator is mounted. Inside the cavity only in the direct neighborhood of the opening/neck pink vortices are visible.

The Howe Model

The idea is to describe the displacement of an infinite thin shear layer of turbulent vortices inside the opening only. The surrounding turbulent flow is considered as an averaged quantity. In figure 3 this modeled shear layer is colored red and blue.

The Howe model describes the Rayleigh conductivity K_R of an opening in grazing, turbulent, two-sided low Mach number flow [4]:

$$\frac{i\omega\rho}{K_R} = \frac{p_+ - p_-}{v_y} = Z_+ - Z_-. \tag{1}$$

ρ, p and v_y are the density, the acoustic pressure, and the acoustic volume flux (through the opening), respectively. Z is the impedance. Quantities above and below the shear layer are denoted by a $+$ and $-$ index, respectively. The qualitative sketch of a displaced shear layer is shown in figure 4.

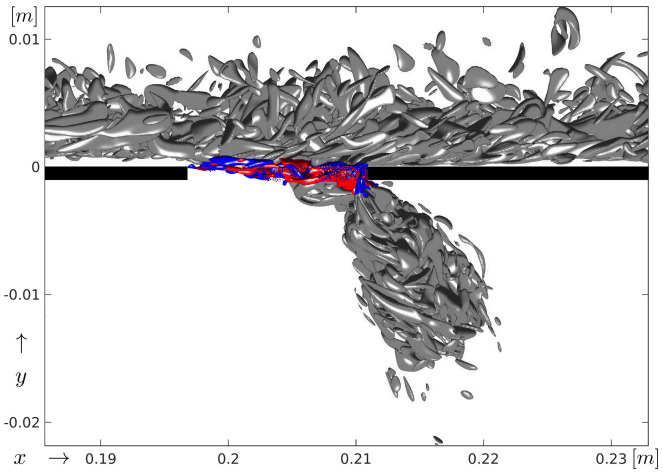

Figure 3: Snapshot of an isosurface of the vorticity. The shear layer at the opening of the Helmholtz resonator is colored.

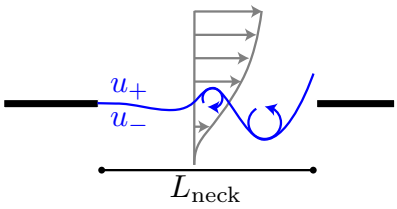

Figure 4: Exemplary sketch of the displacement of a shear layer modeled by Howe [4] for an opening in grazing, two-sided low Mach number flow.

The Rayleigh conductivity K_R of an opening with an arbitrary shape is given by the surface integral [4]

$$K_R = \frac{i\omega\rho}{p_+ - p_-}\int_S v_y dS = \pi L_{\text{neck}}/2 \int_S \zeta' dS, \tag{2}$$

$$\text{with} \quad \zeta' = \frac{\rho\omega^2 (L_{\text{neck}}/2)^2}{\pi}\frac{\zeta}{p_+ - p_-}. \tag{3}$$

ζ is the y-displacement of the vortex sheet. Typically, the complex Rayleigh conductivity K_R is separated into a real and a imaginary part

$$K_R = L_{\text{neck}}\left(\Gamma_R - i\Delta_R\right). \tag{4}$$

Δ_R is proportional to the acoustic energy dissipation rate, $\Delta_R < 0$ implies acoustic excitation.

The Rayleigh conductivity K_R can be calculated directly via ζ' (equation 2) by solving the following integral equation for all x and z locations of the opening surface S:

$$\int_S \frac{\zeta'(\mathbf{x},\mathbf{x}')}{\mathbf{x}-\mathbf{x}'} d\mathbf{x}' + \lambda_1(z)e^{i\sigma_1 x} + \lambda_2(z)e^{i\sigma_2 x} = 1. \tag{5}$$

$$\sigma_{1,2} = \frac{S_\omega}{2}\frac{1 \pm i}{1 \pm i\frac{u_+}{u_-}} \tag{6}$$

are Kelvin-Helmholtz wavenumbers with the Strouhal number $S_\omega = \omega L_{\text{neck}}/u_+$ of the shear layer. The choice of the mean eddy convection velocity $u_\pm$ (see figure 4) is crucial, as it determines which frequency ranges exhibit dissipation of acoustic energy. A general procedure how to define $u_\pm$ is work in progress.

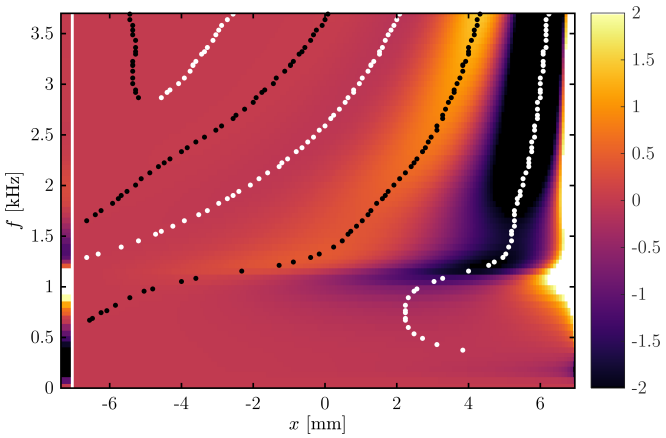

Figure 5: Vortex layer displacement of a rectangular opening ($\mathrm{Im}\,[\zeta']$ of equation 5). The x-axis is the streamwise coordinate. The y-axis is the frequency. The dotted black and white lines mark the maxima and minima of the vortex displacement, respectively. The very left column is the sum of its row.

A discrete numerical solution of equation 5 can be calculated with centroid collocation as suggested in [3]. The ζ'-displacement of the vortex sheet for a rectangular opening (geometry defined in figure 1) is shown in figure 5. As a leading-edge boundary condition, the Kutta condition with $\zeta' = 0$ is applied.

Integration of the Howe Model as an Acoustic Element

The transfer matrix of an linear **acoustic element** [6] is

$$\begin{pmatrix} p_- \\ v_- \end{pmatrix} = M \begin{pmatrix} p_+ \\ v_+ \end{pmatrix}. \tag{7}$$

In order to integrate the Howe model (driven by a pressure source term) inside an acoustic element, J. Golliard [2] formed

$$\begin{pmatrix} p_- \\ v_- \end{pmatrix} = \begin{pmatrix} 1 & Z_{\mathrm{flow}} \\ 0 & 1 \end{pmatrix} \begin{pmatrix} p_+ \\ v_+ \end{pmatrix} + \begin{pmatrix} p_{\mathrm{source}} \\ 0 \end{pmatrix}. \tag{8}$$

Here p_{source} is a source term originating from the turbulent pressure fluctuations of a zero-pressure gradient, turbulent flat plate flow. Z_{flow} is the characteristic impedance of the acoustic element, provided by the Howe model. In the following steps, the impedance Z_{flow} and the Rayleigh conductivity K_R are related. Equation 8 is rearranged to the structure of equation 1

$$\frac{(p_+ + p_{\mathrm{source}}) - p_-}{v_+} = -Z_{\mathrm{flow}}. \tag{9}$$

By comparison with equation 1, the impedance Z_{flow} is newly related by

$$Z_{\mathrm{flow}} = -\frac{i\omega\rho}{K_{\mathrm{flow}}}. \tag{10}$$

K_{flow} is interpreted by J. Golliard [2] as fluid related only

$$\frac{1}{K_{\mathrm{total}}} = \frac{1}{K_{\mathrm{flow}}} + \frac{1}{K_{\mathrm{noflow}}}. \tag{11}$$

First, the total conductivity $K_{\mathrm{total}} = K_R$ and pure acoustical conductivity K_{noflow} have to be known in order to derive K_{flow}. Beside experimental measurement K_{total} and K_{noflow} can be determined by Howe's model, too. Insertion of equation 11 in equation 10 provides

$$Z_{\mathrm{flow}} = i\omega\rho \left(\frac{1}{K_{\mathrm{noflow}}} - \frac{1}{K_{\mathrm{total}}} \right). \tag{12}$$

Separation of the imaginary and real part gives

$$Z_{\mathrm{flow}} = i\,\mathrm{Re}\left[\frac{\omega\rho}{K_{\mathrm{noflow}}} - \frac{\omega\rho}{K_{\mathrm{total}}} \right] - \mathrm{Im}\left[\frac{\omega\rho}{K_{\mathrm{noflow}}} - \frac{\omega\rho}{K_{\mathrm{total}}} \right].$$

Using $Z_0 = \rho c = Y_0 S_0$ the resistance (amplitude alteration) r and reactance (phase shift) δ of the impedance $Z_{\mathrm{flow}} = Y_0(r_{\mathrm{flow}} + ik\delta_{\mathrm{flow}})$ are

$$r_{\mathrm{flow}} = k\,\mathrm{Im}\left[\frac{S_0}{K_{\mathrm{total}}} - \frac{S_0}{K_{\mathrm{noflow}}} \right], \tag{13}$$

$$\delta_{\mathrm{flow}} = \mathrm{Re}\left[\frac{S_0}{K_{\mathrm{noflow}}} - \frac{S_0}{K_{\mathrm{total}}} \right]. \tag{14}$$

$K_{\mathrm{total}} = K_R$ is defined by equation 5; the no-flow conductivity is $K_{\mathrm{noflow}} = \pi S_0 / 2L_{\mathrm{neck}}(\Psi - 2) \in \mathbb{R}$ [4]. Positive reactance $r_{\mathrm{flow}} > 0$ implies acoustic damping analog to $\Delta_R > 0$ and $\mathrm{Im}\,[K_r] < 0$ of equation 4. The sign of the reactance δ_{flow} differs from [5] but is more consistent derived here. Such δ_{flow} agrees with the experimental results of [2] as depicted in figure 6, too.

Figure 6 shows the comparison of experimental measurements with the prediction of the Howe model. The experimental results are valid for a parameter range between $5-45\mathrm{m/s}$ and ratios of $\delta_{99}/L_{\mathrm{neck}} \in [0.7-5]$. Even so the Howe model assumes a low Mach number flow with an infinite thin vortex shear layer the Strouhal numbers of extrema and zero-crossings match very well. This guarantees a correct prediction of dissipative and excited frequencies.

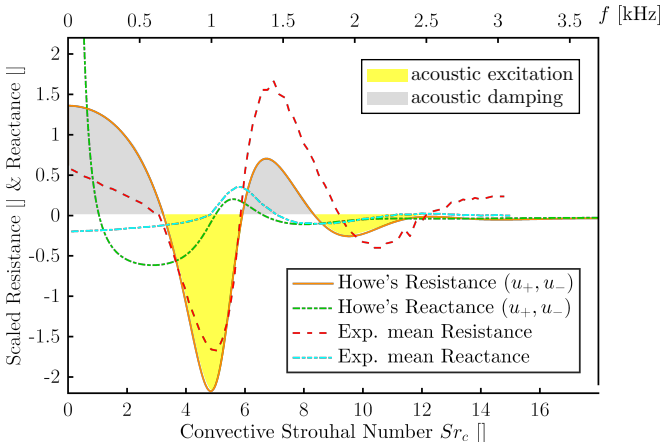

Figure 6: Howe's impedance model vs. experiment by [2].

Sound Prediction Model

p_{source} can be related with p_{mic} at the cavity bottom by inserting Howe's model via Z_{flow} in equation 8. This leads analog to [2] to the final prediction model, which is presented in figure 7. The source term originating from a turbulent flat plate flow is approximated by the Chase model [1]. The first SPL peak of figure 7 at 300 Hz is the Helmholtz base frequency. The second peak is the first vertical (y) cavity mode. The prediction of the extrema's frequencies agrees very well with experiment and DNS results. Only the SPL deviates ±5dB and needs further improvements. Higher cavities modes begin with 1700 Hz. By virtue of simplicity, these modes are not included in the model because they are beyond the typical range of operation.

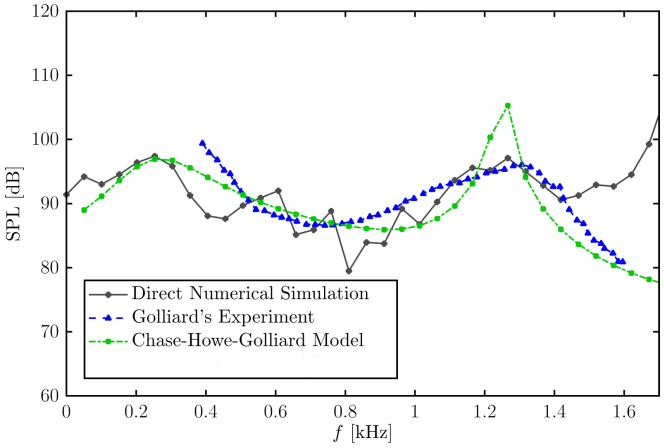

Figure 7: Narrow-band SPL spectrum ($\Delta f = 50$ Hz) centered at the bottom of the Helmholtz cavity (see microphone position in figure 2).

Conclusion

For the first time, we conducted a Direct Numerical Simulation of a three-dimensional Helmholtz resonator, driven by a fully developed turbulent flat plate flow. A new sound prediction model is set up starting with an empirical approach by J. Golliard [2] by integrating the analytical Howe model. The advantage of using the Howe model is the independence of experimental fits and the reduction to only a few characteristic parameters like the opening dimensions and mean convection velocity. This allows a simple application of the prediction model for an industrial liner layout. For the typical range of operation around the Helmholtz base frequency, an agreement between the prediction model, the experimental results [2] and the Direct Numerical Simulation is shown (see figure 7). Furthermore, by looking at the Howe model individually (figure 6), dissipative and excited frequency ranges are identified.

Acknowledgement

The provision of computational resources (ACID11700) by the Federal High-Performance Computing Center Stuttgart (HLRS) are gratefully acknowledged.

References

[1] D. M. Chase. The character of the turbulent wall pressure spectrum at subconvective wavenumbers and a suggested comprehensive model. *Journal of Sound and Vibration*, 112(1):125–147, 1987.

[2] J. Golliard. *Noise of Helmholtz-resonator like cavities excited by a low Mach-number turbulent flow.* PhD thesis, Université de Poitiers, 2002.

[3] S. M. Grace, K. P. Horan, and M. S. Howe. The Influence of Shape on the Rayleigh Conductivity of a Wall Aperture in the Presence of Grazing Flow. *Journal of Fluids and Structures*, 12(3):335–351, 1998.

[4] M. S. Howe. *Acoustics of Fluid-Structure Interactions.* Cambridge monographs on mechanics, 1998.

[5] G. Kooijman, A. Hirschberg, and J. Golliard. Acoustical response of orifices under grazing flow: Effect of boundary layer profile and edge geometry. *Journal of Sound and Vibration*, 315(4-5):849–874, sep 2008.

[6] M. L. Munjal. *Acoustics of Ducts and Mufflers with Application to Exhaust and Ventilation System Design.* Wiley, 1987.

[7] J. Reiss. A Family of Energy Stable, Skew-Symmetric Finite Difference Schemes on Collocated Grids. *Journal of Scientific Computing*, 2015.

[8] J. Sesterhenn. A characteristic-type formulation of the Navier-Stokes equations for high order upwind schemes. *Computers and Fluids*, 30:37–67, 2001.

[9] L. Stein, J. Reiss, and J. Sesterhenn. Numerical simulation of a resonant cavity: Acoustical response under grazing turbulent flow. In *Notes on Numerical Fluid Mechanics and Multidisciplinary Design*, volume 136, pages 671–681. Springer, 2017.